Adv. Polar Upper Atmos. Res., **18**, 87–95, 2004

Research note

Day-to-day variations of migrating semidiurnal tide simulated by a general circulation model

Yasunobu Miyoshi[1] and Hitoshi Fujiwara[2]

[1] *Department of Earth and Planetary Sciences, Faculty of Sciences, Kyushu University, Fukuoka 812-8581*
[2] *Department of Geophysics, Faculty of Science, Tohoku University, Sendai 980-8678*

(Received December 19, 2003; Accepted March 1, 2004)

Abstract: By using a general circulation model, we examine behavior of the migrating semidiurnal tide for equinox during solar cycle minimum and geomagnetically quiet conditions. We investigate day-to-day variations of the migrating semidiurnal tide in the mesosphere and thermosphere, and their relation with the migrating semidiurnal tide generated in the lower atmosphere. The results show that day-to-day variations of the migrating semidiurnal tide are evident from the upper troposphere to the thermosphere. Fluctuations of the migrating semidiurnal tide amplitude with periods of 17–18 and 25 days are found at altitudes from 20 to 200 km height, indicating dynamical coupling between the mesosphere and thermosphere and the lower atmosphere.

key words: semidiurnal tide, dynamical coupling, general circulation model

1. Introduction

The semidiurnal tide is one of the dominant components of the atmospheric motion in the mesosphere and lower thermosphere (MLT). Observational and numerical studies have revealed that the amplitude of the semidiurnal tide has variability with a range from a few days to several years. For example, at middle and high latitudes, the semidiurnal tide amplitude in the MLT is larger in winter than in summer, and a distinct peak of the amplitude appears in September (*e.g.* Manson *et al*., 1989; Tsuda *et al*., 1988). Variations of the semidiurnal amplitude with intraseasonal time scale (10–60 days) are also observed by many radar sites (*e.g.* Pancheva *et al*., 2003).

Several mechanisms are considered to account for the variability of the semidiurnal tide in the MLT. Plausible sources of the variability of the semidiurnal tide are summarized as: (1) variations of forcing in the troposphere and stratosphere, (2) effects of non-migrating tide, (3) effects of nonlinear interaction between the semidiurnal tide and other waves (such as planetary waves and gravity waves), (4) effects of changes in background wind and temperature, (5) changes in solar flux and/or geomagnetic activity.

Miyahara and Miyoshi (1997) showed that the amplitude of the non-migrating semidi-

urnal tide was non-negligible in the MLT (mechanism 2). Pancheva *et al*. (2002) investigated the nonlinear interaction between the 16-day wave and the migrating semidiurnal tide (mechanism 3), Pasncheva *et al*. (2003) indicated a positive correlation between the solar activity and the variability of the semidiurnal tide amplitude. (mechanism 5). Lindzen and Hong (1974), Aso *et al*. (1981) and Riggin *et al*. (2003) showed that changes in the background wind and temperature influenced the semidiurnal amplitude (mechanism 4).

With regard to mechanism 1, Hagan (1996) showed that latent heat release associated with cloudiness and/or rainfall in the troposphere was a plausible source of the variability of the migrating semidiurnal tide in the MLT. However, in Hagan's model, an annual mean distribution of latent heat release is used to investigate forcing of the semidiurnal tide. Effects of day-to-day variations of the general circulation in the troposphere on the semidiurnal tide amplitude in the upper atmosphere have been not examined. Furthermore, observations of day-to-day variations of the semidiurnal tide are restricted in the MLT. Day-to-day variations of the semidiurnal tide in the lower atmosphere (troposphere and stratosphere) and the upper thermosphere are not well known. Thus, mechanisms for the variability of the semidiurnal tide in the MLT are uncertain.

In this study, we investigate day-to-day variations of the migrating semidiurnal tide in the mesosphere and thermosphere, and their relation with the migrating semidiurnal tide generated in the lower atmosphere, by using a general circulation model (GCM) which contains whole atmospheric regions: the troposphere, stratosphere, mesosphere and thermosphere. The descriptions of the GCM used in this study and numerical experiment are presented in Section 2. Results and discussion are presented in Section 3. Summary follows in Section 4.

2. Descriptions of the GCM and numerical experiment

The GCM used in this study is a global spectral model (T21) with 75 vertical levels, and contains the region from the ground surface to the exobase (about 500 km height). The GCM solves the full nonlinear primitive equations for eastward momentum, northward momentum, thermodynamics, continuity and hydrostatics. The detailed descriptions of the GCM are found in Miyoshi and Fujiwara (2003), so that the description of the GCM is briefly mentioned here.

In the troposphere, stratosphere and mesosphere, the GCM has a full set of the physical processes, such as radiation, a boundary layer, hydrology, moist and dry convection and eddy diffusion. Effects of the topography of the surface are also taken into account. The distributions of water vapor and cloud are predicted in the GCM. The distribution of O_3 is climatologically prescribed. Below 95 km height, effects of unsolved orographic and non-orographic gravity wave drags are parameterized by McFarlane (1987) and Lindzen (1981), respectively.

In the thermosphere, the GCM includes schemes for the infrared radiation, absorption of solar extreme ultraviolet (EUV) and ultraviolet (UV) radiations, the ion drag, the Joule heating, the auroral particle precipitation and molecular diffusions of momentum and heat. The neutral composition in the thermosphere is obtained from the empirical model of MSIE90 (Hedin, 1991), and specified as a function of latitude and pressure. The global electron density distribution produced mainly by solar radiation is represented by the Chiu's

empirical model (Chiu, 1975). In addition to electrons obtained by the Chiu's model, electron produced by auroral particles are taken into account as described by Fuller-Rowell and Evans (1987) and Roble and Ridley (1987).

The time integration is conducted for perpetual March equinox conditions during solar cycle minimum (F10.7 cm solar flux=70) and geomagnetically quiet (Ap=4). The integrated data are sampled hourly for the last 300 days after the equilibrium state is realized. By using a space-time Fourier analysis (*e.g.*, Hayashi, 1971), amplitudes of the westward propagating semidiurnal component with zonal wavenumber 2, *i.e.*, the migrating semidiurnal tide, are extracted. Because solar fluxes, the geomagnetic activity and ionospheric parameters are fixed during the numerical experiment, effects of day-to-day variations of solar flux and the geomagnetic activity on the semidiurnal tide are excluded. The season is fixed at equinox, so that day-to-day variations of the zonal mean wind and temperature are small. Thus, effects of variations of the background wind and temperature in the upper mesosphere and thermosphere on the semidiurnal tide are negligibly small.

In this numerical experiment, seasonal variations of the semidiurnal tide are not reproduced, so that the simulated semidoiurnal tide may not resemble the semidiurnal tide in an actual March. However, in order to exclude effects of variations of the back ground wind, it is useful to investigate the behavior of the semidiurnal tide without seasonal changes.

3. Results and discussion

Figure 1 shows the zonal mean zonal wind averaged over 300 days. Eastward winds exist in middle to high latitudes of both hemispheres below 70 km height. The reversal of the zonal wind due to the gravity wave drag (Lindzen, 1981) occurs at 70–80 km height.

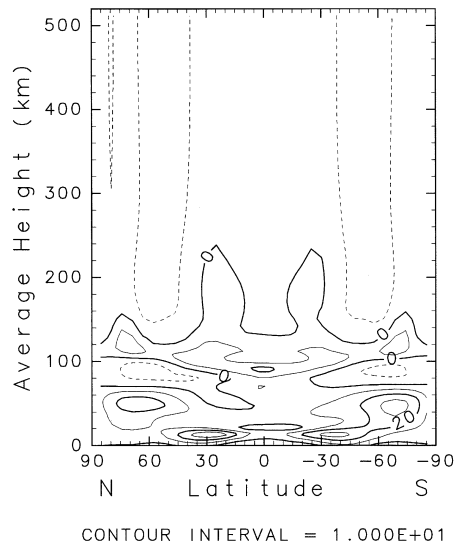

Fig. 1. Latitude-height plot of the zonal mean zonal wind. Contour interval is 10 m/s. Solid and dotted lines represent eastward and westward winds, respectively.

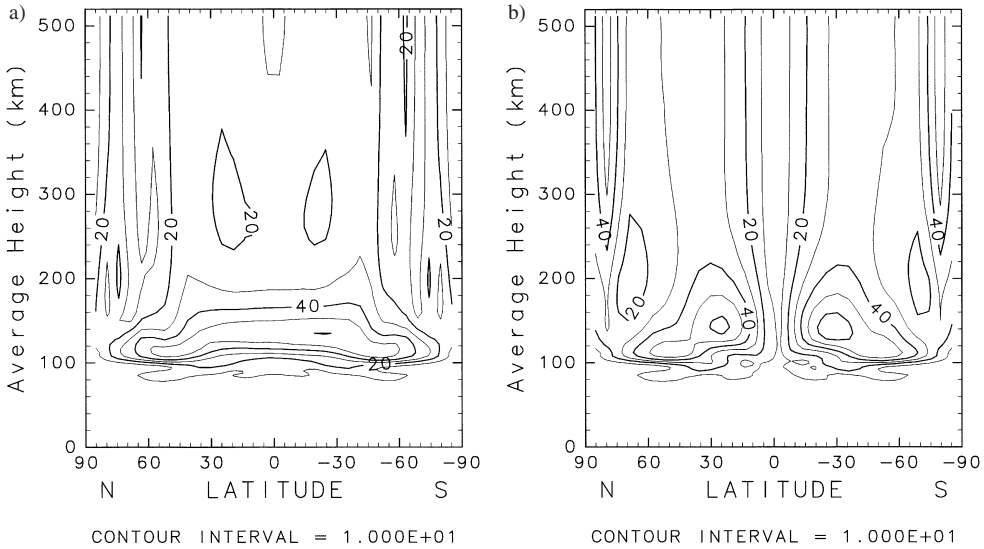

Fig. 2 *(a) Latitude-height plot of the amplitude of the migrating semidiurnal zonal wind component. Contour interval is 10 m/s.*
(b) As in Fig. 2a but for the meridional wind component.

These features are in agreement with those in the real atmosphere (*e.g.*, CIRA86). The zonal mean zonal wind is predominantly eastward between 100 and 140 km height. The zonal mean zonal wind in the upper thermosphere is westward, and the maximum westward wind is located near 60° latitude.

Figure 2a–b show the latitude-height cross section of the amplitude of the migrating semidiurnal tide averaged over 300 days. The amplitude of the zonal and meridional components is 10–15 m/s at 80 km height, and the amplitude between 90–120 km increases rapidly with height. The maximum amplitudes at middle latitudes and at low latitudes are located at 120 and 140 km height, respectively. The maximum value in the lower thermosphere is 60 m/s. The amplitude near the mesopause region is consistent with the radar observations (*e.g.*, Manson *et al.*, 1989), while the amplitude in the lower thermosphere is in good agreement with the observation at Millstone Hill (Goncharenko and Salah, 1998). Generally, due to insufficient global observations of the wind in the thermosphere, evaluation of the model results is restricted. However, present results in the thermosphere are in good agreement with the results obtained by previous simulations (Fesen *et al.*, 1986; Forbes, 1982). Hence, the GCM is quite useful for studying the semidiurnal tide.

Figure 3 show the time-height cross section of deviation of the zonal wind from diurnal mean zonal wind at 0°E and 53°N. This latitude is chosen since the migrating semidiurnal tide in the MLT has maximum around 50° latitude. In the stratosphere and mesosphere, a diurnal wind variation is dominant. As might be expected, the zonal wind has a pronounced semidiurnal variation between 100 and 140 km height, while the *in situ* diurnal tide is dominant above 150 km height.

Here we investigate temporal variability of the migrating semidiurnal tide amplitude at

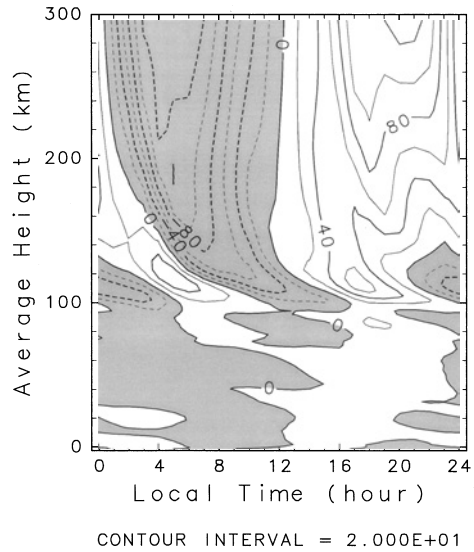

Fig. 3. Longitude-height plot of deviation of the zonal wind from diurnal mean zonal wind at 0°E longitude and 53°N latitude. Contour interval is 20 m/s and shading is used for westward winds.

various heights. Figures 4a–h show time series of the amplitude of the migrating semidiurnal zonal wind component at 53°N at the altitudes of (a) 20 km, (b) 40 km, (c) 60 km, (d) 80 km, (e) 110 km, (f) 150 km, (g) 200 km and (h) 300 km, respectively. The amplitude of the migrating semidiurnal tide is small at 20, 40 and 60 km heights, however, day-to-day variations of the amplitude are clearly seen. The amplitude at 110 km height ranges from 44 to 68 m/s, indicating marked day-to-day variations. The amplitude at 150 km height varies between 19 and 31 m/s, while the amplitudes at 200 and 300 km vary between 12 and 20 m/s and between 10 and 16 m/s, respectively. The amplitude of the migrating semidiurnal tide in the lower thermosphere is more variable than that in the upper thermosphere. Although the neutral composition in the stratosphere, mesosphere and thermosphere, solar fluxes, the geomagnetic activity and ionospheric parameters are fixed during the numerical experiment, day-to-day variations of the migrating semidiurnal tide amplitude are evident in the mesosphere and thermosphere, indicating dynamical coupling between the upper and lower atmosphere. At middle and high latitudes, the amplitudes of the migrating semidiurnal meridional wind and temperature components also have similar day-to-day variations (not shown).

In order to investigate dominant periods of day-to-day variations of the migrating semidiurnal tide amplitude, a spectral analysis is performed. Figure 5 shows power spectra of the migrating semidiurnal zonal wind component at 53°N. Spectral peaks centered at 10–12 days and 17–18 days are evident at all heights ranges. Other distinct peaks at 25 days are found at altitudes from 20 to 200 km. A 40–50 days peak appears at 20, 80, 110 and 300 km height. At other latitudes, similar day-to-day variations of the semidiurnal amplitude are found (not shown).

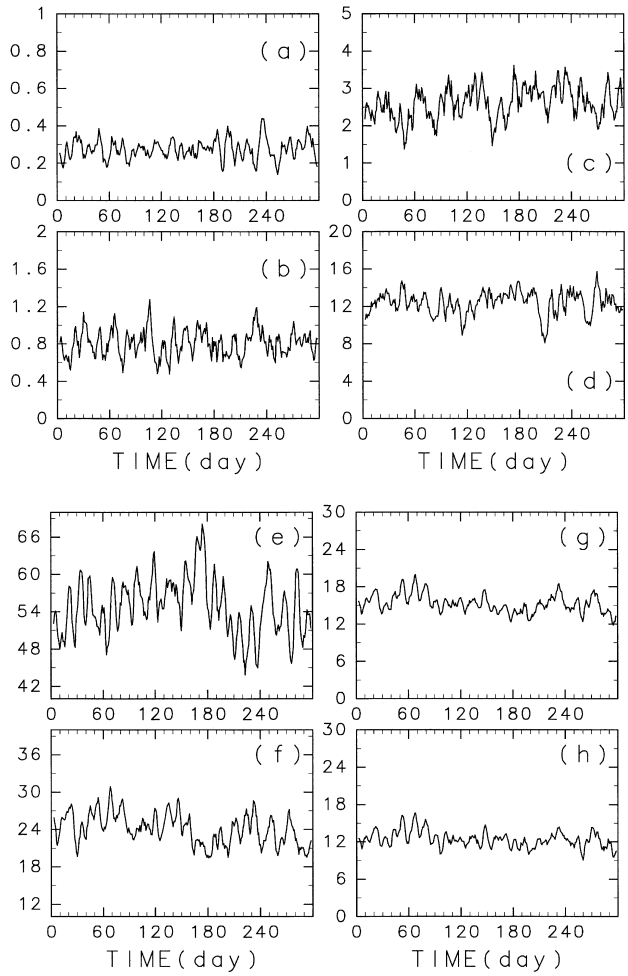

Fig. 4. Time series of amplitudes of the migrating semidiurnal zonal wind component at 53°N. Each panel shows the time series at altitudes of (a) 20 km, (b) 40 km, (c) 60 km, (d) 80 km, (e) 110 km, (f) 150 km, (g) 200 km, (h) 300 km. Units are m/s.

Next, effects of variations of background wind in the upper mesosphere and thermosphere on the tidal variability are examined. Figure 6 shows power spectra of the zonal mean zonal wind at 53°N of 110 km height. Spectral peak centered at 10–12 days is evident, while spectral peaks with 17–18 and 25 days periods are not clear. At 110 km height, day-to-day variations of the semidiurnal tide with 17–18 and 25 days periods are not correlated with variations of the background wind. Similar features are obtained at other heights of the upper mesosphere and thermosphere. Thus, variations of the semidiurnal tide with 17–18 and 25 days periods in the upper mesosphere and thermosphere are generated in the lower atmosphere. Both the semidiurnal tide and the background wind have spectral peaks around 10–12 days period. However, the zonal mean zonal wind at 110 km height ranges

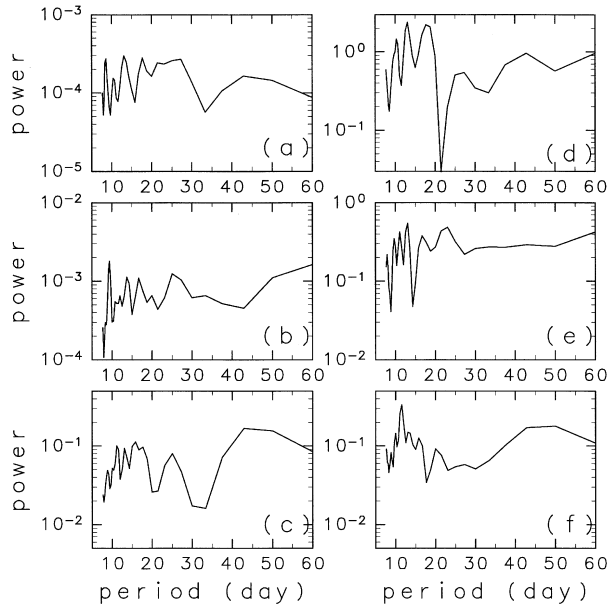

Fig. 5. Power spectra of the migrating semidiurnal zonal wind amplitude at 53°N at altitudes of (a) 20 km, (b) 40 km, (c) 80 km, (d) 110 km, (e) 200 km and (f) 300 km. Units are $m^2/s^2 \cdot day$.

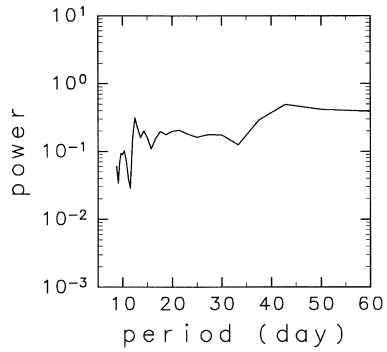

Fig. 6. Power spectra of the zonal mean zonal wind amplitude at 53°N of 110 km height. Units are $m^2/s^2 \cdot day$.

from 3 to 10 m/s, and is much smaller than variations of the semidiurnal tide at 110 km (Fig. 4e). It is considered that effects of background wind variations with 10–12 days period on the semidiurnal tide at 110 km are negligibly small.

By using meteor radar, Pancheva *et al*. (2003) showed that the semidiurnal amplitude in the MLT fluctuated with 10, 15–18, 25–28 days periods. These observed variations of the semidiurnal amplitude are similar to the present results. Moreover, Pancheva *et al*. (2003) found that variations with 10, 15–18, 25–28 days were observed simultaneously in the total ozone and in the semidiurnal amplitude. Most ozone molecules are concentrated below 30

km height, where the photochemical lifetime of ozone (several weeks) is longer than the time scale of advection (a few days). Thus, the changes in the total ozone are controlled by variations of the general circulation in the lower stratosphere. These results imply that the semidiurnal tide in the MLT is influenced by variations of the general circulation in the lower atmosphere, and consistent with the present result.

In the present study, day-to-day variations of the migrating semidiurnal tide amplitude are evident from the tropopause to the upper thermosphere. The fact that fluctuations of the migrating semidiurnal amplitude with periods of 10–12, 17–18 and 25 days are found at altitudes from 20 to 200 km shows that the semidiurnal migrating tide in the mesosphere and thermosphere is influenced by the semidiurnal migrating tide generated in the lower atmosphere. The distributions of water vapor and cloud in the troposphere have day-to-day variations, and these variations influence forcing of the semidiurnal tide due to the absorption of the solar radiation in the troposphere. Hagan (1996) suggested that latent heat release associated with cloudiness and rainfall was another source for the migrating semidiurnal tide. Thus, variability of water vapor and cloud affects excitation of the migrating semidiurnal tide in the troposphere. These results suggest that day-to-day variations of the general circulation in the troposphere influence the migrating semidiurnal tide amplitude in the mesosphere and thermosphere.

4. Summary

By using the GCM which contains the region from the ground surface to the exobase, day-to-day variations of the migrating semidiurnal tide amplitude are investigated. Although the neutral composition in the stratosphere, mesosphere and thermosphere, solar fluxes, the geomagnetic activity and ionospheric parameters are fixed during the numerical experiment, day-to-day variations of the migrating semidiurnal tide amplitude are evident from the tropopause to the upper thermosphere. The fact that fluctuations of the migrating semidiurnal amplitude with periods of 17–18 and 25 days are found at altitudes from 20 to 200 km height shows that the migrating semidiurnal tide in the mesosphere and thermosphere is influenced by the migrating semidiurnal tide generated in the lower atmosphere.

In the next step, we will evaluate the tidal signatures in the upper atmosphere in the presence of day-to-day variations of the solar EUV and UV fluxes, geomagnetic activity, ionospheric parameters. Then, the tidal waves in whole atmospheric regions and the coupling processes between the lower and upper atmosphere will be understood more quantitatively.

Acknowledgments

We thank Prof. T. Aso for his helpful discussions. The GFD-DENNOU Library was used for drawing figures. This research was financially supported by a Grant-in-Aid for Scientific Research from the Ministry of Education, Culture, Sports, Science and Technology, Japan. We also thank the referees for their valuable comments on our original manuscript.

The editor thanks Dr. T. Aso and another referee for their help in evaluating this paper.

References

Aso, T., Nonoyama, T. and Kato, S. (1981): Numerical simulation of semidiurnal atmospheric tides. J. Geophys. Res., **86**, 11388–11400.

Chiu, Y.T. (1975): An improved phenomenological model of ionospheric density. J. Atmos. Terr. Phys., **37**, 1563–1570.

Fesen, C.G., Dickinson, R.E. and Roble, R.G. (1986): Simulation of the thermospheric tides at equinox with the National Center for Atmospheric Research thermospheric general circulation model. J. Geophys. Res., **91**, 4471–4489.

Forbes, J.M. (1982): Atmospheric Tides 2. The solar and lunar semidiurnal components. J. Geophys. Res., **87**, 5241–5252.

Fuller-Rowell, T.J. and Evans, D.S. (1987): Height-integrated Pederson and Hall conductivity patterns inferred from the TIROS-NOAA satellite data. J. Geophys. Res., **92**, 7606–7618.

Goncharenko, L.P. and Salah, J.E. (1998): Climatology and variability of the semidiurnal tide in the lower thermosphere over Millstone Hill. J. Geophys. Res., **103**, 20715–20726.

Hagan, M.E. (1996): Comparative effects of migrating solar souces on tidal signatures in the middle and upper atmosphere. J. Geophys. Res., **101**, 21213–21222.

Hayashi, Y. (1971): A generalized method of resolving disturbances into progressive and retrogressive waves by space Fourier and time cross-spectral analysis. J. Meteorol. Soc. Jpn., **49**, 125–128.

Hedin, A.E. (1991): Extension of the thermosphere model into the middle and lower atmosphere. J. Geophys. Res., **96**, 1159–1172.

Lindzen, R.S. (1981): Turbulence and stress owing to gravity wave and tidal breakdown. J. Geophys. Res., **86**, 9707–9714.

Lindzen, R.S. and Hong, S. (1974): Effects of mean winds and horizontal temperature gradients on solar and lunar semidiurnal tides in the atmosphere. J. Atmos. Sci., **31**, 1421–1446.

McFarlane, N.A. (1987): The effect of orographically excited gravity wave drag on the general circulation of the lower stratosphere and troposphere. J. Atmos. Sci., **44**, 1775–1800.

Manson, A.H., Meek, C.E., Teitelbaum, H., Vial, F., Schminder, R., KürSchner, D., Smith, M.J., Fraser, G.J. and Clark, R.R. (1989): Climatology of semidiurnal and diurnal tides in the middle atmosphere (70–100 km) at middle latitudes (40–55°). J. Atmos. Terr. Phys., **51**, 579–593.

Miyahara, S. and Miyoshi, Y. (1997): Migrating and non-migrating atmospheric tides simulated by a middle atmosphere general circulation model. Adv. Space Res., **20**, 1201–1207.

Miyoshi, Y. and Fujiwara, H. (2003): Day-to-day variations of migrating diurnal tide simulated by a GCM from the ground surface to the exobase. Geophys. Res. Lett., **30**, 1789, doi:10.10129/2003GL017695.

Pancheva, D., Mitchell, N., Clark, R.R., Drobjeva, J. and Lastovicka, J. (2002): Variability in the maximum height of the ionospheric F2-layer over Millstone Hill (September 1998–March 2000); influence from below and above. Ann. Geophys., **20**, 1807–1819.

Pancheva, D., Mitchell, N., Middleton, H. and Muller, H. (2003): Variability of the semidiurnal tide due to fluctuations in solar activity and total ozone. J. Atmos. Sol.-Terr. Phys., **65**, 1–19.

Riggin, D.M., Meyer, C.K., Fritts, D.C., Jarvis, M.J., Murayama, Y., Singer, W., Vincent R.A. and Murphy, D.J. (2003): MF radar observations of seasonal variability of semidiurnal motions in the mesosphere at high northern and sourthern latitudes. J. Atmos. Sol.-Terr. Phys., **65**, 483–493.

Roble, R.G. and Ridley, E.C. (1987): An auroral model for the NCAR thermospheric general circulation model (TGCM). Ann. Geophys., **54**, 369–382.

Tsuda, T., Kato, S., Manson, A.H. and Meek, C.E. (1988): Characteristics of semidiurnal tides observed by the Kyoto meteor radar and Saskatoon medium-frequency radar. J. Geophys. Res., **93**, 7027–7036.